CHEMICAL ENGINEERING TRANSACTIONS
VOL. 39, 2014
A publication of AIDIC
The Italian Association of Chemical Engineering
www.aidic.it/cet
Guest Editors: Petar Sabev Varbanov, Jiří Jaromír Klemeš, Peng Yen Liew, Jun Yow Yong

ISBN 978-88-95608-30-3; **ISSN** 2283-9216
DOI: 10.3303/CET1439048

Assessment of Working Fluid Mixtures for Solar Organic Rankine Cycles

Paschalia Mavrou[a], Athanasios I. Papadopoulos[a*], Mirko Stijepovic[b], Panos Seferlis[c,a], Patrick Linke[b], Spyros Voutetakis[a]

[a]Chemical Process and Energy Resources Institute, Centre for Research and Technology-Hellas, 57001 Thermi, Greece
[b]Chemical Engineering Department, Texas A&M University at Qatar, P.O. Box 23874, Doha, Qatar
[c]Department of Mechanical Engineering, Aristotle University of Thessaloniki, 54124 Thessaloniki, Greece
spapadopoulos@cperi.certh.gr

This work investigates the performance of binary working fluid mixtures in a low temperature solar Organic Rankine Cycle (ORC) system including heat storage. Conventional mixtures widely considered in published literature are compared with optimum mixtures previously obtained using a computer-aided molecular design method in Papadopoulos et al. (2013). The system performance is investigated for a real solar radiation profile for an entire year of operation. Inclusive, steady-state mathematical models are used for the simulation of both the solar collectors and the ORC. The effects of different mixtures on several important system operating parameters are investigated. Results indicate that mixtures at different compositions and concentrations may have a significantly different performance in terms of parameters such as generated work, required collector aperture area and so forth. Neopentane- based mixtures appear as promising candidates of high overall performance for solar ORCs.

1. Introduction

ORC systems have become a field of intense research as a power generation technology from low enthalpy heat sources due to their easy implementation and high efficiency.Their operation is based on heat extraction using an appropriate working fluid which is vaporised and subsequently expanded in a turbine to produce work that can be used in numerous applications such as desalination (Li et al., 2013) and electricity generation (Quoilin et al., 2011) to name a few. Solar ORCs are particularly interesting since different types of solar collectors can be used resulting in different heat carrier temperature ranges. Various types of collectors have been studied in literature such as flat plate collectors (FPC) (Wang et al., 2013), parabolic trough collectors (PTC) (Quoilin et al., 2011) or compound parabolic concentrators (CPC) (Gang et al., 2011). Clearly, selecting the working fluid and the solar collector as well as the system configuration is crucial since they impact on the overall system performance. Such impacts have been analysed for important working fluid properties in Stijepovic et al. (2012). Several of them were used as performance criteria by Papadopoulos et al. (2010a) in the first reported implementation of a computer-aided molecular design (CAMD) approach for ORC working fluids. This work was recently extended by Papadopoulos et al. (2013) in a novel approach for the design of ORC working fluid mixtures.
To date solar ORC utilizing pure working fluids have been widely investigated (Wang et al., 2013), due to their simpler thermodynamic and operating characteristics compared to mixed working fluids. An important limitation of pure working fluids is their constant temperature profile during phase change (Papadopoulos et al., 2013). The pinch point encountered at the evaporator and the condenser gives rise to large temperature differences at one end of the heat exchanger leading to high irreversibility. To increase power generation most investigated solar ORC employ PTC or CPC as they facilitate the development of higher temperatures even at low solar radiation. The simpler FPC produce lower outlet heat carrier temperatures resulting in lower power generation. Using mixtures as working fluids in FPC-based solar ORC may

Please cite this article as: Mavrou P., Papadopoulos A.I., Stijepovic M., Seferlis P., Linke P., Voutetakis S., 2014, Assessment of working fluid mixtures for solar organic rankine cycles, Chemical Engineering Transactions, 39, 283-288 DOI:10.3303/CET1439048

considerably improve system efficiency as the emergence of the Pinch can be avoided. The latter is possible due to the variable temperature profile of mixtures during phase change, avoiding pinches and resulting in lower irreversibility and higher cycle exergy efficiency. To date, few reported works have addressed the use of mixtures in solar ORC (e.g., Wang et al., 2010), considering mostly conventional and widely investigated fluids. For the first time in solar ORCs this work compares conventional with novel mixtures designed for optimality (Papadopoulos et al. 2013). The mixtures are investigated for year-round solar irradiation conditions, as opposed to most publications which consider constant irradiation.

2. Models and methods

This work investigates the performance of a solar ORC with heat storage in view of different working fluid mixtures (Figure 1). An inclusive model is developed for the FPC system taking into account detailed heat flows and design equipment characteristics. This is complemented by a detailed ORC model emulating all heat transfer and power generation features, capturing the non-ideal mixture behavior. Employing a heat storage tank is vital for the system since it helps minimize frequent ORC start-ups and maintain a continuous power output, addressing solar intermittence. The employed models are presented below.

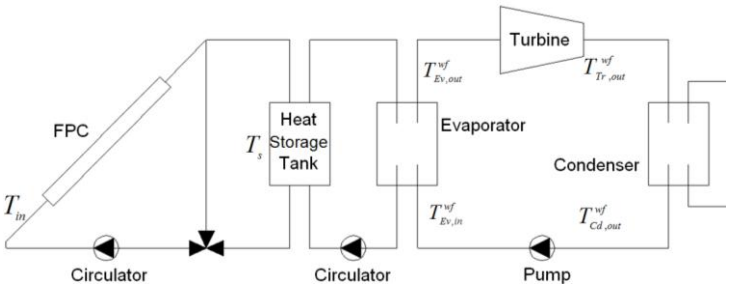

Figure 1: Layout of a solar ORC

2.1 Flat Plate collector model

The useful energy output Q_u (W) of a flat plate solar collector in steady state conditions is the difference between absorbed solar radiation and thermal losses (Duffie and Beckman, 1991):

$$Q_u = A_c[I_s - U_L(T_{pm} - T_{amb})] \tag{1}$$

where A_c (m^2) is the solar collector area, U_L (W/m^2 K) is the overall heat loss coefficient, T_{pm} (K) and T_{amb} are the mean absorber and ambient temperatures. The incident solar radiation I_s (W/m^2) is calculated as:

$$I_s = I_b R_b (\tau\alpha)_b + I_d (\tau\alpha)_d \left(\frac{1+\cos(\beta)}{2}\right) + \rho_g (I_b + I_d)(\tau\alpha)_g \left(\frac{1-\cos(\beta)}{2}\right) \tag{2}$$

where R_b is the ratio of solar radiation on an inclined surface to that of a horizontal surface in the northern hemisphere, $(\tau\alpha)$ is the transmittance absorbance product, I is the radiation and subscripts b, d, g stand for beam, diffuse and ground. The collector overall heat loss coefficient U_L is the sum of top U_t, back U_b and side loss Ue coefficients. Top loss coefficient is given from the following equation (Wang et al., 2013):

$$U_t = \left[\frac{N}{\frac{C}{T_{pm}}\left(\frac{T_{pm}-T_{amb}}{N+f}\right)^{0.33}} + \frac{1}{h_w}\right]^{-1} + \frac{\sigma\left(T_{pm}+T_{amb}\right)\left(T_{pm}^2+T_{amb}^2\right)}{\left[\varepsilon_p + 0.05\left(1-\varepsilon_p\right)\right]^{-1} + \frac{2N+f-1}{\varepsilon_g} - N} \tag{3}$$

where N is the number of glass covers, h_w (W/m^{2}K) is the wind convective heat transfer coefficient, σ (W/m^{2}K^4) is the Stephan-Boltzmann coefficient, ε_p is the absorber plate emissivity and ε_g is the glass emissivity. Bottom loss coefficient is described by the following equation:

$$U_b = k_b / t_{b,ins} \tag{4}$$

where k_b (W/m K) is the conductivity and $t_{b,ins}$ (mm) is the thickness of the insulation for the surface in question. Term U_e, namely the edge loss coefficient is calculated as follows:

$$U_e = k_e t_{coll} Per / (t_{e,ins} A_c) \quad (5)$$

Similarly, k_e is the conductivity and $t_{e,ins}$ is the thickness of the insulation. Also t_{coll} is the collector thickness and Per (mm) its perimeter. The collector useful energy output is also expressed as follows:

$$Q_u{}' = F_R A_c \left[I_s - U_L \left(T_{in} - T_{amb} \right) \right] \quad (6)$$

where F_R is the heat removal factor and T_{in} (K) is the fluid temperature at the collector inlet. The calculations are performed by setting $Q_u = Q_u'$.

2.2 Heat storage tank model

Considering that the fluid (e.g. water) inside the tank is fully mixed with fluid returning from the evaporator and collector outlet, the heat storage tank is modeled by the following energy balance:

$$\left(MC_p \right) \frac{dT_s}{dt} = \dot{Q}_u - \dot{Q}_{loss} - \dot{Q}^{Ev} \quad (7)$$

where $\dot{Q}_u$ (W) is the rate of heat gain from the collector, $\dot{Q}_{loss}$ is the rate of convection losses to the ambient, $\dot{Q}^{Ev}$ is the rate of heat transferred to the ORC via the evaporator and M (kg) is the mass of the fluid inside the heat storage tank. Since the data for I are hourly averaged, to obtain the value for $\dot{Q}_u$ during the one hour time period Q_u has to be multiplied by 3600 s/h.

2.3 ORC model

The ORC utilizes an organic mixture for the recovery of solar heat and consists of an evaporator (Ev), a turbine (Tr), a condenser (Cd) and a pump (Pm). To estimate the maximum P_{max} (bar) and minimum P_{min} pressures the mixture is assumed saturated vapour at the Ev outlet. P_{max} is assumed equal to the dew pressure $P_{dew,wf}$.of the working fluid (wf) at the Ev outlet. At the Cd outlet the wf is assumed in a state of saturated liquid, therefore P_{min} is considered equal to the bubble point pressure $P_{bub,wf}$. The estimation of $P_{dew,wf}$ and $P_{bub,wf}$ is performed through vapour liquid equilibrium calculations using an equation of state (EoS). The wf mass flow rate is evaluated from a heat and mass balance in the Ev. It is assumed that the pinch occurs in the Ev when the wf starts to boil. Therefore the temperature $T^{ev,hc}$ corresponding to the bubble point temperature $T_{bub}^{Ev,wf}$ of the wf is calculated as (Papadopoulos et al., 2013):

$$T^{Ev,hc} = T_{bub}^{Ev,wf} + \Delta T_{\min} \quad (8)$$

In the Ev isobaric heat addition and isothermal phase change are assumed and the absorbed heat is described by the following equation:

$$\dot{Q}^{Ev} = \dot{m}_f^{wf} \left(H_{Ev,out}^{wf} - H_{Ev,in}^{wf} \right) \quad (9)$$

where $\dot{m}_f^{wf}$ (kg/s) is the wf mass flow rate and H_{Ev}^{wf} (kJ/kg) is the enthalpy at inlet and outlet conditions of the Ev. The equation is similar for the Cd. In the Tr ideal conditions are assumed, thus adiabatic and isentropic expansion is employed and the produced work (kW) is calculated as follows:

$$\dot{W}^{Tr} = \eta^{Tr} \dot{m}_f^{wf} \left(H_{Tr,out}^{wf} - H_{Ev,out}^{wf} \right) \quad (10)$$

where η^{Tr} is the Tr isentropic efficiency. Finally, the Pm is assumed to operate under adiabatic and isothermal conditions and the consumed work is obtained from the following equation:

$$\dot{W}^{Pm} = \dot{m}_f^{wf} \left(1/\rho^{wf} \right) \left(1/\eta^{Pm} \right) \left(P_{\max} - P_{\min} \right) \quad (11)$$

where ρ^{wf} is the average wf density (kg/m^3) between Pm inlet and outlet and η^{Pm} is the Pm isentropic efficiency. In Eq(11) the pressure unit is N/m^2.

2.4 Evaluation parameters

The thermodynamic performance criteria used for evaluation of the system include thermal and exergy efficiency. The ORC thermal efficiency is calculated as follows:

$$\eta_{th,ORC} = \left(\left| \dot{W}^{Tr} \right| - \dot{W}^{Pm} \right) / \dot{Q}^{Ev} \quad (12)$$

The ORC exergy efficiency is calculated as follows:

$$\eta_{II,ORC} = \left(\left|\dot{W}^{Tr}\right| - \dot{W}^{Pm}\right) / \left[m^{hc}\left[\left(H^{hc} - H^{0,hc}\right) - T^{0,hc}\left(S^{hc} - S^{0,hc}\right)\right]\right] \quad (13)$$

where m^{hc} is the heat carrier mass flow rate, namely the water in the storage tank sub-system, H^{hc} and S^{hc} (kJ/kg K) is the heat carrier's enthalpy and entropy respectively at storage tank temperature and $H^{0,hc}$ and $S^{0,hc}$ is the heat carrier's enthalpy and entropy respectively at nominal temperature $T^{0,hc}$ equal to 298 K.

3. Implementation

3.1 Selection of mixtures

The layout of Figure 1 is used to test several binary mixtures previously proposed for solar ORCs. Those fluids are compared with several novel ORC mixtures previously obtained using a CAMD approach (Papadopoulos et al., 2013). All molecules are alkanes, fluorinated alkanes or fluoromethoxy-alkanes due to the wide public availability of data for the prediction of their properties using group contribution methods. Such methods include generalized models to predict molecular properties required for the subsequent evaluation of mixture properties through cubic EoS. The selected mixtures are shown in Table 1.

Table1: Proposed mixtures

	Component 1	Component 2
E1[a]	Isopentane	Isobutane
E2[a]	Isopentane	Hexane
E3[a]	Isopentane	Isohexane
E4[a]	Pentane	Hexane
E5[b]	Butane	Pentane
E6[b]	Isobutane	Pentane
M1[c]	1,1,1,3,3,3-hexafluoro-propane	1-fluoromethoxy-2,2,2-trifluoro-methyl-ethane
M2[c]	Neopentane	1,1,1-trifluoro-2-trifluoro-methyl-butane
M3[c]	Neopentane	1,1,1-trifluoropentane
M4[c]	1,1,1-trifluoro-2-trifluoromethylpropane[c]	2,2-difluoro-hexane

[a]Chys et al., 2012;[b] Liu et al., 2014;[c]Papadopoulos et al., 2013

3.2 Case study details

Solar irradiation, wind velocity and ambient temperature are considered using actual hourly averaged data representing a typical year in Xanthi, Greece. The solar field consists of 6 loops, each of 11 collectors of aperture area A_c=2 m^2 installed in series. The ε_g is 84 % and the ε_p is 4 %. The insulation in the collector is stone wool of 40 mm. The collector tilt angle is 45^o. The capacity of the heat storage tank is 3,960 L. The ORC is deactivated when the storage tank temperature T_s drops below 80 ^{o}C. The $T_{s,max}$ is assumed 95 ^{o}C to avoid phase change. Condensation temperature $T_{out}^{Cd,wf}$ is assumed 30 ^{o}C. The $\Delta T_{\min}$ in the Ev is 10 K. The η^{Pm} is 50 % and the η^{Tr} is 70 %. All mixtures are investigated at concentrations 0.1-0.9 mole fraction.

To evaluate the performance of the mixtures this work considers an inclusive objective function combining several important ORC operating parameters. The simulations span an entire year hence one of the objectives is to maintain a prolonged operating duration t_{op}. Work produced with respect to maximum work available for the considered temperature range is represented by $\eta_{II,ORC}$, while $\eta_{th,ORC}$ represents the conversion of thermal energy to work. Both these indices are maximized. High $\dot{m}_f^{wf}$ and $P_{\max}$ are often associated with increased equipment costs hence they are minimized. All these parameters are included scaled in the following objective function (*OF*) which is maximized:

$$\max J = t_{op} \cdot \eta_{II,ORC} \cdot \eta_{th,ORC} / \left(\dot{m}_f^{wf} \cdot P_{\max}\right) \quad (14)$$

4. Results and discussion

Table 2 illustrates important ORC operating parameters for the top ranking mixtures obtained using Eq(14). For the considered *OF* the mixtures employed in published literature are outperformed by those of Table 2. This behaviour is expected considering that mixtures M1-M4 were designed for low temperature applications such as geothermal power generation (Papadopoulos et al., 2010b). The optimum mixture is M1 at a concentration of 60 % Neopentane (all reported concentrations refer to the first molecule). Note that several mixtures of the same compositions (i.e. same molecules) are repeated in the top set at different concentrations. This is also expected as the employed *OF* captures optimum parameter trade-

offs. All optimum mixtures operate between approximately 300 and 400 h/y while the net power produced from the ORC is in the order of 1 kW. The $P_{\max}$ and $P_{\min}$ are low, while operation is above one 1 bar.

Table2: Optimum mixtures for solar ORC

Mixture	t_{op} (h)	$\lvert\dot{W}^{Tr}\rvert - \dot{W}^{Pm}$ (10^{-1}kW)	$\dot{m}_f^{wf}$ (10^{-1}kg/s)	$P_{\max}^{ORC}$ (bar)	$P_{\min}^{ORC}$ (bar)	$\eta_{th,ORC}$ (%)	$\eta_{II,ORC}$ (%)	J
60 % M1	309	10.64	1.15	3.60	1.77	4.21	17.28	1.585
50 % M1	299	10.51	1.12	3.10	1.55	4.03	17.12	1.568
70 % M1	341	10.70	1.10	4.31	1.98	4.66	17.20	1.363
60 % M4	327	9.90	1.05	2.29	1.06	4.11	15.99	1.310
40 % M1	310	10.43	1.04	2.72	1.33	4.10	17.00	1.299
40 % M2	325	10.31	1.04	2.17	1.02	4.23	16.68	1.128
80 % M1	414	10.11	0.95	5.36	2.18	5.39	15.95	0.942

The association of operating duration with the average produced power is shown in Figure 2a which includes both designed mixtures (e.g. M1, M2 and M3) and conventional ones (e.g. E1, E5, E6). Figure 1a forms an optimum set of mixtures (Pareto front) illustrating the trade-off between operating duration and produced power. Mixtures with long operating duration result in reduced power production and vice versa. Mixtures that generate increased power, may satisfy a higher load demand due to their higher exergy efficiency, and result in fast deactivation of the ORC because of the fast drop in the heat storage tank temperature. Some mixtures appear towards both ends of the diagram. For example, E5 presents a long operating duration (823 h) and relatively low produced power (0.54 kW) at a 90 % concentration, while it also operates for 576 h producing 0.835 kW at 30 % concentration. This is an indication that Butane at high concentration results in longer operation and lower power generation compared to having Pentane at higher concentration. A similar trend is observed for all the mixtures depicted in Figure 2a. Mixtures within the circle generate the highest amount of power during the year (i.e. most kWh). Those are E5 at 30-80 % and E1 at 40 %. Few of the mixtures in Figure 2a appear in Table 2, because it was developed using different evaluation criteria. For example, the maximum ORC pressure for mixtures E1, E5, E6 is higher than those of Table 2 while their exergy efficiency is lower hence they are not included in Table 2. While the results obtained using Eq(14) as a performance criterion provide an inclusive consideration of different parameters, results in Figure 2 address specific operating issues and provide significant insights.

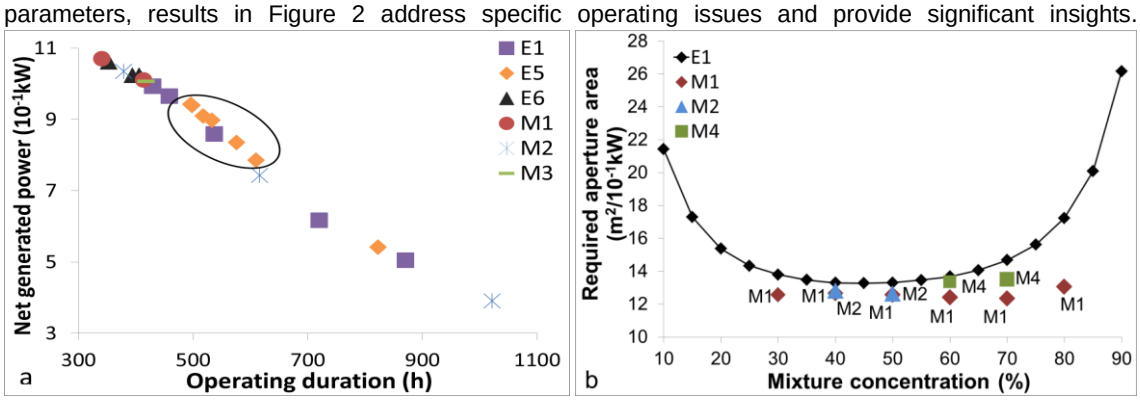

Figure2: a) Trade-offs between net generated power and operating duration, b) Effect of mixture concentration on required aperture area.

Figure 2b shows the collector aperture area required to generate 1 kW of power with respect to mixture concentration. The performance of M1, M2 and M4 is compared with E1. As additional quantity of a second component is introduced in an existing pure component the required thermal energy to generate 1 kW in the ORC is reduced, hence lower solar collector aperture area is required.

Figure 3a compares the exergy and thermal efficiency characteristics of the mixtures in Table 2 with E1. Each pair of markers corresponding to the same concentration (vertically) indicates one of the mixtures M1, M2, M4 at different concentrations. All optimum mixtures present a higher exergy and a lower thermal efficiency than E1. Figure 3b illustrates the mass flowrate and the maximum pressure of mixtures with respect to concentration, using E1 as a reference mixture. For E1, as additional quantity of the more volatile isobutane is added the maximum pressure is increased. The same trend holds for the other mixtures. Each pair of markers corresponding to the same concentration (vertically) indicates one of M1, M2, M4. For M1, M2 and M4 markers square, triangle and diamond correspond to mass flowrate values,

while markers circle, star and dash correspond to pressure values. The mass flowrate is lower for concentrations close to pure components and for the three optimum mixtures it is much higher than E1. This shows that the employed *OF* reflects the observed trade-off between the desired higher exergy efficiency and the undesired higher mass flowrate.

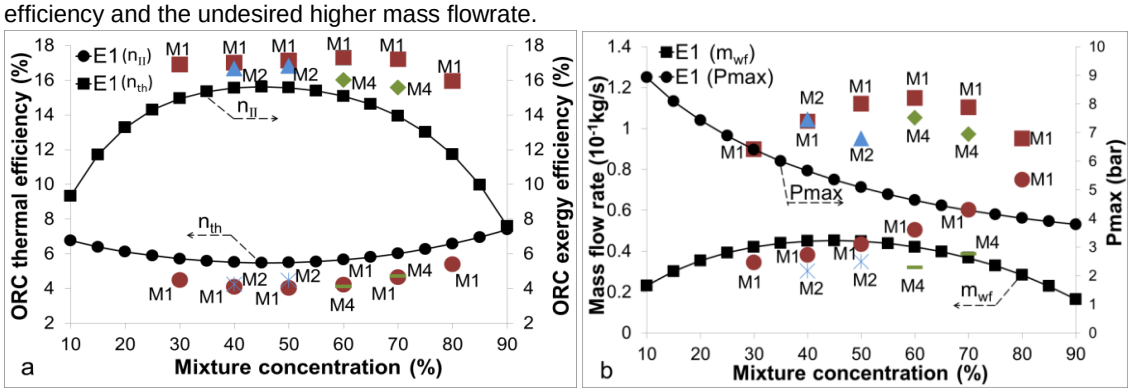

Figure 3: Effect of mixture concentration on a) ORC thermal and exergy efficiency, b) ORC mass flowrate and maximum pressure

5. Conclusions

The present work assessed the performance of a low temperature solar ORC system over an entire year under variable compositions of several binary working fluids. A detailed model was developed for the system comprising a flat plate collector, a heat storage tank and an ORC considering heat and mass flows as well as design characteristics. The performance of the system under different working fluids was evaluated using an objective function optimizing several ORC characteristics. The Neopentane - 1,1,1-trifluoropentane mixture appears to be optimum for many concentrations but among them 60 % Neopentane qualifies as most efficient.

References

Chys M., van den Broek M., Vanslambrouck B., De Paepe M., 2012, Potential of zeotropic mixtures as working fluids in organic Rankine cycles, Energy, 44, 623-632.

Duffie J.A., Beckman W.A., 1991, Solar engineering of thermal processes, 2nd ed., Willey, New York, USA.

Gang P., Jing L., Jie J., 2011, Design and analysis of a novel low-temperature solar thermal electric system with two-stage collectors and heat storage units, Renew Energ, 36, 2324-2333.

Li C., Kosmadakis G., Manolakos D., Stefanakos E., Papadakis G., Goswam, D.Y., 2013, Performance investigation of concentrating solar collectors coupled with a transcritical organic Rankine cycle for power and seawater desalination co-generation, Desalination, 318, 107-117.

Liu Q., Duan Y., Yang Z., 2014, Effect of condensation temperature glide an the performance of organic Rankine cycles with zeotropic mixture working fluids, Appl Energ, 115, 394-404.

Papadopoulos A.I., Stijepovic M., Linke P., 2010a, On the systematic design and selection of optimal working fluids for Organic Rankine Cycles, Appl Therm Eng, 30, 760-769.

Papadopoulos A.I., Stijepovic M., Linke P., Seferlis P., Voutetakis S, 2010b Power generation from low enthalpy geothermal fields by design and selection of efficient working fluids for Organic Rankine Cycles, Chemical Engineering Transactions, 21, 61-66.

Papadopoulos A.I., Stijepovic M., Linke P., Seferlis P., Voutetakis S., 2013, Toward optimum working fluid mixtures for organic Rankine cycles using molecular design and sensitivity analysis, Ind Eng Chem Res, 52 (34), 12116-12133.

Stijepovic M., Linke P., Papadopoulos A.I., Grujic A., 2012, On the role of working fluid properties in Organic Rankine Cycle performance, Appl Therm Eng, 36, 406-413.

Quoilin Q., Orosz M., Hemond H., Lemort V., 2011, Performance and design optimization of a low-cost organic Rankine cycle for remote power generation, Sol Energy, 85, 955-966.

Wang M., Wang J., Zhao Y., Zhao P., Dai Y., 2013, Thermodynamic analysis and optimization of a solar-driven regenerative organic Rankine cycle (ORC) based on flat-plate solar collectors, Appl Therm Eng, 50, 816-825.

Wang J.L., Zhao L., Wand X.D., 2010, A comparative study of pure and zeotropic mixtures in low temperature solar Rankine cycle, Appl Energ, 87, 3366-3373.